

# Conformational equilibria of polar and charged flexible polymer chains in water<sup>☆</sup>

H.S. Ashbaugh<sup>a,b</sup>, E.W. Kaler<sup>a</sup>, M.E. Paulaitis<sup>c,\*</sup>

<sup>a</sup>Department of Chemical Engineering and Center for Molecular and Engineering Thermodynamics, University of Delaware, Newark, DE 19716, USA

<sup>b</sup>Department of Chemical Engineering, Princeton University, Princeton, NJ 08544, USA

<sup>c</sup>Department of Chemical Engineering, The Johns Hopkins University, Baltimore, MD 21218-2694, USA

## Abstract

Continuum model predictions of the conformational equilibria of idealized polar and charged linear polymers in water are compared to complementary simulations in explicit water. The continuum model of hydration predicts with reasonable accuracy the conformational dependence of the hydration free energy of these solutes observed in the simulations. However, a prerequisite for accurate predictions is the optimization of the phenomenological parameters inherent to the continuum model using the simulation results for a subset of the solutes, in this case the uncharged polymer and two amphiphilic polymer chains with a single positive or negative charge on one terminal group. Our results demonstrate that the continuum model can be used to discriminate among the conformational preferences for different sequences of backbone charges. Finally, an unexpected finding of this study is the stabilization in water of the more compact conformations of the polymer chains with a fixed dipole moment. The driving force for this behavior is greater than the hydrophobic driving force and is electrostatic in nature. © 2001 Elsevier Science Ltd. All rights reserved.

**Keywords:** Polymer; Hydration; Conformational equilibrium

## 1. Introduction

In a previous study [1], we considered whether a continuum model of hydration optimized to reproduce vacuum-to-water transfer free energies also describes the conformational equilibria of the same solutes at infinite dilution in water. Three model oligomers were studied: a simple hydrophobic tetramer, modeled as butane, and two amphiphilic tetramers, modeled as butane with either a positive or negative charge ( $\pm 1e$ , where  $e$  is the fundamental unit of electrostatic charge) on one terminal methyl group. Continuum model predictions for vacuum-to-water transfer free energies and the conformational dependence of the free energies of hydration were compared to results obtained from explicit water simulations.

One conclusion drawn from this study was that the continuum model fails to predict both the transfer free energies and the conformational dependence of the hydration free

energies for these solutes. Specifically, the continuum model parameters (i.e., the hydrophobic free energy/surface area coefficient and the Born radii of the charged methyl groups) fit to the transfer free energies are significantly different from those obtained by fitting the conformational dependence of the free energies of hydration. This observation has important implications for continuum model descriptions of macromolecular self-assembly in aqueous solutions, since the phenomenological parameters inherent to the continuum model are typically optimized to reproduce transfer free energies for a representative set of model solutes and then applied to macromolecular self-assembly in aqueous solution.

A question that naturally arises from our previous study is whether the continuum model parameters, fit instead to the conformational dependence of the hydration free energy for a subset of solutes, can be used to predict the conformational equilibria for a much wider range of polar and charged polymeric solutes in aqueous solution. To address this question, we extend our previous analysis to consider polar and charged tetramers with positive or negative charges assigned to several constituent groups along the polymer backbone. Continuum model predictions of the conformational dependence of the hydration free energies for these solutes are compared to complementary explicit water simulations.

<sup>☆</sup> This paper was originally submitted to *Computational and Theoretical Polymer Science* and received on 19 October 2000; received in revised form on 2 January 2001; accepted on 2 January 2001. Following the incorporation of *Computational and Theoretical Polymer Science* into *Polymer*, this paper was consequently accepted for publication in *Polymer*.

\* Corresponding author. Tel.: +1-410-516-7170; fax: +1-410-516-5510.  
E-mail address: michaelp@jhu.edu (M.E. Paulaitis).

## 2. Theoretical background

### 2.1. Conformational equilibrium

The normalized probability for observing a solute with a single conformational degree of freedom, taken to be the backbone dihedral angle  $\phi$ , in a given conformation is

$$P(\phi) = \frac{\exp[-\beta\Delta A(\phi)]}{\int_0^{2\pi} \exp[-\beta\Delta A(\phi)] d\phi} \quad (1)$$

where  $\beta^{-1} = kT$  is the thermal energy, and  $\Delta A(\phi)$  is the change in free energy as a function of  $\phi$ . This expression is readily generalized to solutes with multiple conformational degrees of freedom. In aqueous solution,  $\Delta A(\phi)$  has contributions from the intramolecular potential energy,  $\Delta E_{\text{int}}(\phi)$ , and the free energy of hydration,  $\Delta A_{\text{hyd}}(\phi)$ . The first contribution can be determined from ab initio quantum mechanical [2] or molecular mechanical calculations [3]. This work focuses on the determination of  $\Delta A_{\text{hyd}}(\phi)$  using two fundamentally different theoretical approaches: explicit water simulations and continuum models of hydration.

A simple measure of the effect of hydration on solute conformational equilibrium is the *trans*  $\leftrightarrow$  *gauche* equilibrium constant:

$$K \equiv \frac{x_g}{x_t} = \frac{2 \int_0^{2\pi/3} P(\phi) d\phi}{\int_{2\pi/3}^{4\pi/3} P(\phi) d\phi} \quad (2)$$

where  $x_i$  is the fraction of *gauche* ( $\phi \approx 60$  and  $300^\circ$ ) or *trans* ( $\phi = 180^\circ$ ) conformers. In vacuum, the conformational probability depends solely on  $\Delta E_{\text{int}}(\phi)$ . Using the bond torsional energy defined by Eq. (3) in the following section, the *trans*  $\leftrightarrow$  *gauche* equilibrium constant for butane in vacuum at  $25^\circ\text{C}$  is 0.469, corresponding to a *trans/gauche* population ratio of 68.1%/31.9%. The hydration of butane is expected to shift this equilibrium towards the *gauche* conformer ( $K > 0.469$ ), consistent with the notion that hydrophobic interactions tend to minimize the solvent accessible surface area of the solute. The role of polar electrostatic interactions is more complex.

### 2.2. Explicit water simulations

For notational convenience, we denote an uncharged methyl group as Z, and  $+1e$  or  $-1e$  charged methyl groups as P or M, respectively. A tetramer with a  $+1e$  charge on one terminal methyl group, a  $-1e$  charge on the adjacent methylene group, and the remaining groups uncharged would be designated PMZZ. The tetramers studied in order of increasing number of charges on the solute were ZZZZ, PZZZ, MZZZ, PMZZ, MPZZ, PMPZ, MPMZ, and PMPM. Lennard–Jones (LJ) interactions for the methyl and methylene groups were modeled using the OPLS united atom parameters for butane [4]. The bond torsional energy

of butane is expressed as a truncated Fourier series

$$\Delta E_{\text{int}}(\phi) = \frac{1}{2} V_1 (1 + \cos \phi) + \frac{1}{2} V_2 (1 - \cos 2\phi) + \frac{1}{2} V_3 (1 + \cos 3\phi) \quad (3)$$

whose coefficients ( $V_1 = 1.522$  kcal/mol,  $V_2 = -0.315$  kcal/mol, and  $V_3 = 3.207$  kcal/mol) were fit to the results of MM2 molecular mechanics calculations [3,5]. The LJ interaction parameters for the charged tetramers were taken to be the same as those for an uncharged tetramer. Water was modeled using the simple point charge (SPC) potential [6]. The LJ parameters for solute–water interactions were obtained using geometric mean combining rules,  $\sigma_{\text{sw}} = (\sigma_{\text{ss}}\sigma_{\text{ww}})^{1/2}$  and  $\epsilon_{\text{sw}} = (\epsilon_{\text{ss}}\epsilon_{\text{ww}})^{1/2}$ , where  $\sigma$  and  $\epsilon$  are the LJ diameter and well-depth, respectively. Minimum image LJ interactions were truncated on a site-by-site basis at half the simulation box length.

Electrostatic interactions were evaluated using the generalized reaction field (GRF) method introduced by Hummer et al. [7]. It has been shown that hydration free energies and pair correlation functions determined from the GRF method compare quantitatively with rigorous Ewald summation simulations if ‘self-interactions’ are taken into account [7–10]. The GRF electrostatic energy of a system of  $N_w$  SPC water molecules and a single solute molecule is

$$\begin{aligned} E_{\text{GRF}} = & \sum_{1 \leq i < j \leq N_w} \sum_{\alpha=1}^3 \sum_{\beta=1}^3 q_{w_\alpha} q_{w_\beta} \varphi_{\text{GRF}}(r_{i_\alpha j_\beta}) \\ & + \sum_{i=1}^{N_w} \sum_{\alpha=1}^{\nu} \sum_{\beta=1}^3 q_{s_\alpha} q_{w_\beta} \varphi_{\text{GRF}}(r_{s_\alpha i_\beta}) \\ & + \frac{1}{2} \sum_{i=1}^{N_w} \sum_{\alpha=1}^3 \sum_{\beta=1}^3 q_{w_\alpha} q_{w_\beta} \psi_{\text{GRF}}(r_{i_\alpha i_\beta}) \\ & + \frac{1}{2} \sum_{\alpha=1}^{\nu} \sum_{\beta=1}^{\nu} q_{s_\alpha} q_{s_\beta} \psi_{\text{GRF}}(r_{s_\alpha s_\beta}) \end{aligned} \quad (4)$$

where  $\varphi_{\text{GRF}}$  is the effective GRF electrostatic pair potential,  $\psi_{\text{GRF}}$  is the self-interaction potential,  $q_{w_\alpha}$  and  $q_{s_\alpha}$  are the water and solute charges, and  $\nu$  is the number of charged solute sites. A factor of  $1/4\pi\epsilon_0$  is neglected in Eq. (4) for notational simplicity, where  $\epsilon_0$  is the permittivity of free space.  $\varphi_{\text{GRF}}$  depends only on the minimum image separation,  $r$ , between charges and has the form of a screened Coulombic interaction cut-off at a separation of  $r_c$  [8,9].

$$\varphi_{\text{GRF}}(r) = \frac{1}{r} \left(1 - \frac{r}{r_c}\right)^4 \left(1 + \frac{8r}{5r_c} + \frac{2r^2}{5r_c^2}\right) \Theta(r_c - r) - \frac{\pi r_c^2}{5L^3} \quad (5)$$

where  $\Theta(x)$  is the Heaviside unit-step function. An electrostatic cutoff of  $r_c = L/2$  is used throughout this work. The

Table 1  
Continuum model parameters optimized to the conformational equilibrium of tetramers ZZZZ, PZZZ, and MZZZ [1]

| Parameter | Description                                      | Value                         |
|-----------|--|-------------------------------|
| $\Gamma$  | Hydrophobic free energy/surface Area coefficient | 109 cal/(mol $\text{\AA}^2$ ) |
| $R_p$     | Water probe radius                               | 1.40 $\text{\AA}$             |
| $R_0$     | vdW radius of an uncharged methyl group          | 1.90 $\text{\AA}$             |
| $R_+$     | Radius of a cationic methyl group                | 2.01 $\text{\AA}$             |
| $R_-$     | Radius of an anionic methyl group                | 1.78 $\text{\AA}$             |

self-interaction potential is defined as  $\psi_{\text{GRF}}(r) = \varphi_{\text{GRF}}(r) - 1/r$  [8,9].

The GRF self-interaction energy of a rigid molecule is constant and affects only the absolute magnitude of the electrostatic energy, not the outcome of a Monte Carlo (MC) simulation move. This condition holds for SPC water since the OH bond length and the HOH bond angle are fixed. Thus, the total water self-interaction energy, the third term in Eq. (4), is constant, independent of the configuration of water molecules in the simulation. For a flexible molecule, however, the self-interaction energy may change with its conformation. Since the intramolecular charge separations for all of the charged tetramers, except PMPM, are independent of the solute conformation, the self-interaction energy does not affect their conformational equilibrium. For PMPM, the distance between the opposing charged groups changes with its conformation. Therefore, the solute self-interaction energy contributes  $q_{s_1}q_{s_4}\psi_{\text{GRF}}(r_{s_1s_4}(\phi))$  to the change in conformational energy in solution.

Canonical ensemble MC simulations [11] were carried out for a single tetramer in 212 SPC water molecules at 25°C and a water density of 0.997 g/cm<sup>3</sup>. A simulation run consisted of 40,000 MC passes for equilibration, followed by 160,000 MC passes for sampling (1 MC pass = 212 attempted water moves and four attempted solute moves). Preferential sampling [12] was applied to enhance water moves in the vicinity of the tetramer. The relative free energy difference between the solute in a reference conformation defined by  $\phi$ , and perturbed conformation defined by  $\phi + \delta\phi$ , was evaluated using the free energy perturbation (FEP) formula [13]:

$$\Delta A(\phi \rightarrow \phi + \delta\phi) = -k_B T \ln \langle \exp\{-\beta[E(\phi + \delta\phi) - E(\phi)]\} \rangle_\phi \quad (6)$$

where the brackets  $\langle \dots \rangle_\phi$  denote averaging over molecular configurations generated while holding the solute fixed in  $\phi$ . Twelve tetramer conformations were simulated from  $\phi = 7.5$  to 172.5° in increments of 15°. Conformations corresponding to 180° <  $\phi$  < 360° need not be considered due to symmetry. Perturbations of  $\delta\phi = \pm 7.5^\circ$  were performed

every MC pass. Smaller perturbations of  $\delta\phi = \pm 3.75^\circ$  yielded identical free energies. Therefore, only results from the larger perturbations are reported. A simulation uncertainty was estimated by dividing each simulation run into five equivalent blocks that were assumed to be statistically independent of one another.

### 2.3. Continuum model of hydration

In the continuum model,  $\Delta A_{\text{hyd}}$  is evaluated at fixed solute conformation by dividing the hydration process into three steps [1,14]. In the first step, charges on the solute, initially in vacuum, are turned off to give  $\Delta A_{\text{vac}}(q_s \rightarrow 0)$ . In the second step, the uncharged solute is transferred from vacuum into water to give the free energy of hydrophobic hydration,  $\Delta A_{\text{H}\phi}$ . Finally, the charges are turned back on in aqueous solution to give  $\Delta A_{\text{aq}}(0 \rightarrow q_s)$ . The sum of these three contributions is the hydration free energy:  $\Delta A_{\text{hyd}} = \Delta A_{\text{vac}}(q_s \rightarrow 0) + \Delta A_{\text{H}\phi} + \Delta A_{\text{aq}}(0 \rightarrow q_s)$ , where the individual contributions are calculated as follows.

The free energy of hydrophobic hydration is calculated from the following linear relationship between the free energy and solute surface area:

$$\Delta A_{\text{H}\phi} = \Gamma \mathcal{A} + b \quad (7)$$

where  $\mathcal{A}$  is the surface area,  $\Gamma$  is the hydrophobic free energy/surface area coefficient, and  $b$  is the free energy of hydration for a point solute ( $\mathcal{A} = 0$ ). The value of  $b$  is inconsequential to conformational equilibrium, since it cancels in the normalization of  $P(\phi)$ . Simulations of butane, pentane, and hexane in SPC water have shown that the van der Waals (vdW) surface provides a reasonable, quantitative description of the conformational dependence of  $\Delta A_{\text{H}\phi}$  [1,15]. The vdW radius of the uncharged methyl group and  $\Gamma$  are given in Table 1.

Electrostatic contributions to the free energy of hydration are calculated by treating the solute as a charged cavity embedded in a structureless macroscopic dielectric medium. At the solute boundary, defined by the molecular surface [16], the dielectric constant changes discontinuously from an interior value,  $\epsilon_i$ , to an exterior value,  $\epsilon_e = 1$  or 65 (dielectric constant of SPC water [9]) depending on whether the solute is in vacuum or aqueous solution. To compare the continuum model calculations with our simulation results, we take  $\epsilon_i = 1$  since the simulations neglect molecular polarizability. The electrostatic potential is determined by solving Poisson's equation at a point  $\mathbf{r}$  within the solute cavity [17,18]:

$$\Phi(\mathbf{r}) = \frac{1}{4\pi\epsilon_i\epsilon_0} \sum_{\alpha=1}^v \frac{q_{s_\alpha}}{|\mathbf{r} - \mathbf{r}_\alpha|} + \Phi_{\text{surf}}(\mathbf{r}) \quad (8)$$

where  $\mathbf{r}_\alpha$  denotes the solute charge positions. The first term on the right-hand side of Eq. (8) is due to direct Coulombic interactions with the fixed solute charges, and  $\Phi_{\text{surf}}(\mathbf{r})$  is the potential due to interactions with the induced surface charge density in the solvent at the solute boundary. The

Table 2  
*trans* ↔ *gauche* equilibrium constants. The numbers in parentheses are the simulation uncertainties reported to one standard deviation

| Solute           | $K_{\text{simulation}}$                        | $K_{\text{continuum}}$ |
|------------------|--|------------------------|
| ZZZZ (in vacuum) | 0.469  | N/A                    |
| ZZZZ             | 0.570 (0.031)                                  | 0.596                  |
| PZZZ             | 0.0925 (0.0157)                                | 0.0919                 |
| MZZZ             | 0.0768 (0.0106)                                | 0.0723                 |
| PMZZ             | 1.65 (0.29)                                    | 1.69                   |
| MPZZ             | 1.08 (0.17)                                    | 1.18                   |
| PMPZ             | 0.0808 (0.0110)                                | 0.0710                 |
| MPMZ             | 0.0533 (0.0110)                                | 0.0384                 |
| PMPM             | $2.28 \times 10^{-7}$ ( $1.8 \times 10^{-8}$ ) | $1.26 \times 10^{-7}$  |

electrostatic free energy of transferring the solute from vacuum to aqueous solution is

$$\Delta A_{\text{elec}} = \frac{1}{2} \sum_{\alpha=1}^{\nu} q_{s_{\alpha}} [\Phi_{\text{surf}}(\mathbf{r}_{\alpha}, \epsilon_e = \epsilon_{\text{aq}}) - \Phi_{\text{surf}}(\mathbf{r}_{\alpha}, \epsilon_e = 1)] \quad (9)$$

where  $\Delta A_{\text{elec}} = \Delta A_{\text{vac}}(q_s \rightarrow 0) + \Delta A_{\text{aq}}(0 \rightarrow q_s)$ . The direct Coulombic interaction contribution does not appear in Eq. (9) since it is the same in vacuum and aqueous solution.

For molecular solutes, Poisson's equation is solved numerically using the boundary element method (BEM) [17,19–22]. The molecular surface of the solute was discretized using Zauhar's SMART (Smooth Molecular Triangulator) program [23]. An angle parameter of  $25^\circ$  was used to triangulate the solute surface. Using a finer element size (i.e., a smaller angle parameter) did not affect the results significantly. The SMART discretized surface was the input for the BEM Poisson equation solver [24]. The water probe radius,  $R_p$ , and Born radii of the uncharged,  $R_0$ , and charged,  $R_+$  and  $R_-$ , methyl groups that define the solute molecular

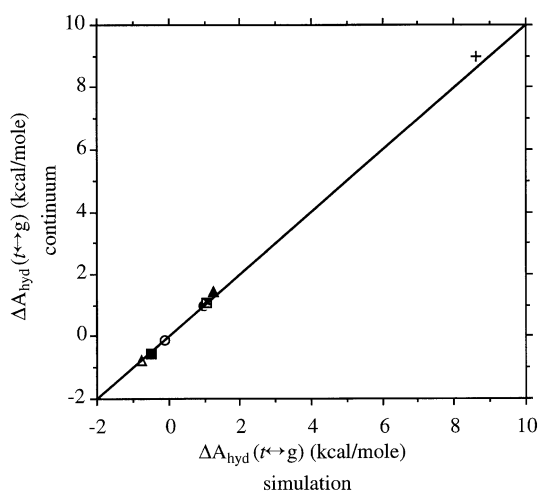


Fig. 1. Comparison of  $\Delta A_{\text{hyd}}(t \leftrightarrow g)$  evaluated by simulation and the continuum model. The diagonal line corresponds to perfect agreement between the simulation and continuum predictions. The symbols denote the tetramers: (○) ZZZZ; (●) PZZZ; (□) MZZZ; (△) PMZZ; (■) MPZZ; (×) PMPZ; (▲) PMPZ; and (+) PMPM.

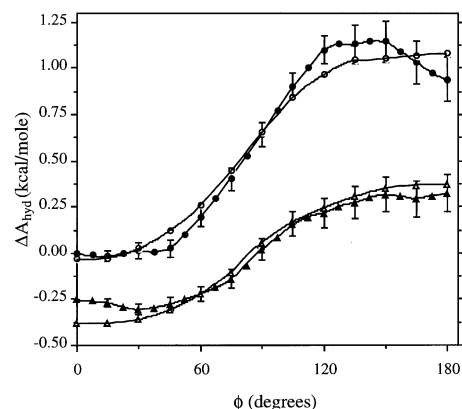


Fig. 2.  $\Delta A_{\text{hyd}}$  of PMZZ and MPZZ as a function of  $\phi$ . The closed (●) and open (○) circles are the simulation and continuum model results for PMZZ. The closed (▲) and open (△) triangles are the simulation and continuum model results for MPZZ, respectively. The simulation results for  $\Delta A_{\text{hyd}}$  are referenced to  $\Delta A_{\text{hyd}}(0^\circ) = 0$  and  $-0.25$  kcal/mol for PMZZ and MPZZ, respectively. The continuum predictions have been shifted by an arbitrary constant that minimizes the mean square difference between the simulation and continuum results for  $\Delta A_{\text{hyd}}$ . The simulation error bars correspond to one standard deviation.

surface are given in Table 1.  $R_+$  and  $R_-$  were optimized in our previous study [1] to reproduce the conformational dependence of  $\Delta A_{\text{hyd}}$  for tetramers PZZZ and MZZZ.

### 3. Results and discussion

#### 3.1. *trans* ↔ *gauche* Equilibria

The *trans* ↔ *gauche* equilibrium constants for all eight tetramers are given in Table 2. The difference in hydration free energy between the *trans* and *gauche* conformations of a tetramer is related to the ratio of the equilibrium constant in aqueous solution to that in vacuum as follows [25]:

$$\Delta A_{\text{hyd}}(t \leftrightarrow g) = -k_B T \ln \left( \frac{K_{\text{aq}}}{K_{\text{vac}}} \right). \quad (10)$$

A negative  $\Delta A_{\text{hyd}}(t \leftrightarrow g)$  indicates that hydration favors the *gauche* conformation, while a positive value indicates that hydration favors the *trans* conformation. Continuum model predictions are plotted against the simulation results for  $\Delta A_{\text{hyd}}(t \leftrightarrow g)$  in Fig. 1. The diagonal line in this plot represents a perfect agreement between these two values. Overall, the continuum model predictions are excellent. The root mean square difference is 0.15 kcal/mol for values of  $\Delta A_{\text{hyd}}(t \leftrightarrow g)$  that range from  $-8.61$  (PMPM) to 0.75 (PMZZ) kcal/mol, or  $\sim 16kT$ . Ranking  $\Delta A_{\text{hyd}}(t \leftrightarrow g)$  yields: PMZZ < MPZZ < ZZZZ < PZZZ < MZZZ  $\approx$  PMPZ < PMPZ < PMPM. The general pattern that emerges from this ranking when the tetramers are grouped based on number of charges,  $\nu$ , is:  $\nu = 2 < \nu = 0 < \nu = 1 \leq \nu = 3 < \nu = 4$ . Within each grouping, the  $\Delta A_{\text{hyd}}(t \leftrightarrow g)$  for a tetramer with a positive terminal group is less than

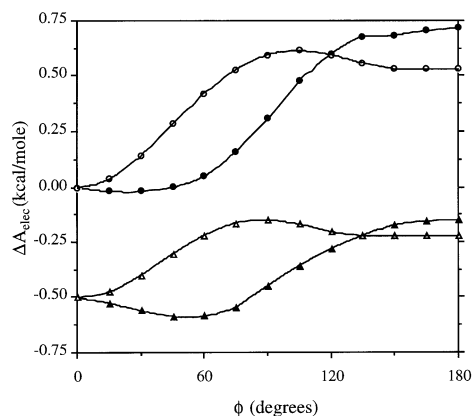


Fig. 3.  $\Delta A_{\text{elec}}$  of PMZZ and MPZZ as a function of  $\phi$  calculated from the continuum model. The closed (●) and open (○) circles are the molecular and spherical representations of PMZZ. The closed (▲) and open (△) triangles are the molecular and spherical representations of MPZZ, respectively.  $\Delta A_{\text{elec}}$  is referenced to  $\Delta A_{\text{elec}}(0^\circ) = 0$  and  $-0.25$  kcal/mol for PMZZ and MPZZ, respectively.

$\Delta A_{\text{hyd}}(t \leftrightarrow g)$  for the tetramer with a negative terminal group; e.g., PMPZ < MPMZ.

### 3.2. PMZZ and MPZZ

The simulation results for  $\Delta A_{\text{hyd}}(\phi)$  of the two dipolar tetramers, PMZZ and MPZZ, are shown in Fig. 2 as a function of  $\phi$ . In both cases, the hydration free energy of the *trans* conformation is higher than that of the *cis* conformation. Moreover,  $K_{\text{PMZZ}} > K_{\text{MPZZ}} > K_{\text{ZZZZ}}$ . This observation is counterintuitive and indicates that electrostatic interactions in the absence of a conformationally dependent dipole moment [26] can stabilize the more compact conformation of the polymer, an effect typically associated with a poor

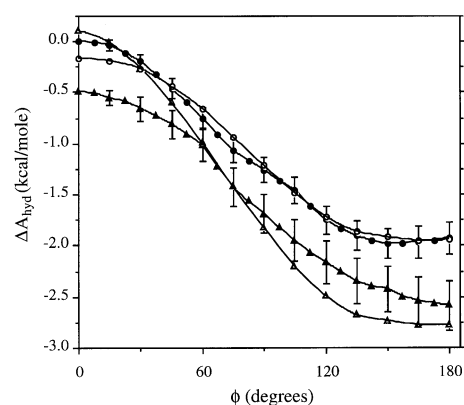


Fig. 4.  $\Delta A_{\text{hyd}}$  of PMPZ and MPMZ as a function of  $\phi$ . The closed (●) and open (○) circles are the simulation and continuum model results for PMPZ. The closed (▲) and open (△) triangles are the simulation and continuum model results for MPMZ. The simulation results for  $\Delta A_{\text{hyd}}$  are referenced to  $\Delta A_{\text{hyd}}(0^\circ) = 0$  and  $-0.5$  kcal/mol for PMPZ and MPMZ, respectively. The continuum predictions have been shifted by an arbitrary constant that minimizes the mean square difference between the simulation and continuum results for  $\Delta A_{\text{hyd}}$ . The simulation error bars correspond to one standard deviation.

solvent or hydrophobic interactions. The continuum model also predicts the destabilization of the *trans* conformation relative to the *cis* conformation, as shown in Fig. 2.

The electrostatic destabilization of the *trans* conformation of the dipolar tetramers can be understood using Kirkwood's continuum model of solvation [27], which assumes a spherical solute, thereby simplifying the theoretical treatment. The electrostatic contribution to the free energy of hydration can be expanded analytically in terms of the moments of the solute charge distribution. Truncating this expansion at the level of dipolar interactions gives

$$\Delta A_{\text{elec}} = -\frac{\mu^2}{4\pi\epsilon_0 r^3} \left( \frac{\epsilon_{\text{aq}} - 1}{2\epsilon_{\text{aq}} + 1} \right) \quad (11)$$

where  $\mu$  is the solute dipole moment, and  $r$  is the radius of the solute cavity. Eq. (11) suggests that changes in either  $\mu$  or the solute volume  $V_s = 4\pi r^3/3$  affects  $\Delta A_{\text{elec}}$ . For many solutes, minor changes in conformation dramatically change  $\mu$ , while  $V_s$  is relatively unaffected. Moreover, the impact of changing  $\mu$  is magnified since  $\Delta A_{\text{elec}}$  is proportional to  $\mu^2$ . Thus, electrostatic contributions to conformational equilibria usually are assumed to depend on  $\mu$  alone [18,26,28]. However, for these dipolar tetramers,  $\mu$  is independent of  $\phi$ . Thus, only changes in  $V_s$  affect  $\Delta A_{\text{elec}}$ . In particular, if  $V_s$  increases for the *cis*  $\rightarrow$  *trans* conformational transition, then  $\Delta A_{\text{elec}}$  similarly increases.

$\Delta A_{\text{elec}}$  for PMZZ and MPZZ calculated using both Eqs. (8) and (9), and Eq. (11) are shown in Fig. 3. To calculate the free energy using Eq. (11), the tetramers are treated as spherical cavities with  $V_s$  equal to the molecular volume (the volume subtended by the molecular surface) and  $\mu = 7.4$  Debye, the dipole moment of both tetramers. The quantitative agreement between the molecular and spherical representations is poor for both tetramers. This poor agreement is attributed to the simplified description of the solute surface used in Eq. (11). Nonetheless, Eq. (11) does predict that the net electrostatic free energy of the *trans* conformation is greater than that of the *cis* conformation, and  $\Delta A_{\text{elec}}(0^\circ \rightarrow 180^\circ) = \Delta A_{\text{elec}}(180^\circ) - \Delta A_{\text{elec}}(0^\circ)$  evaluated using either description is similar in magnitude for each tetramer. Furthermore,  $\Delta A_{\text{elec}}(0^\circ \rightarrow 180^\circ)$  for PMZZ is approximately twice that for MPZZ based on either description. We conclude, therefore, that the observed destabilization of the *trans* conformation relative to the *cis* conformation is due to an increase in volume of the low dielectric solute cavity corresponding to the *cis*  $\rightarrow$  *trans* conformational transition.

### 3.3. PMPZ and MPMZ

The conformational dependence of the hydration free energies for the PMPZ and MPMZ tetramers are shown in Fig. 4. For both charged tetramers the *trans* conformation is favored relative to the *cis* conformation, similar to the behavior observed for PZZZ and MZZZ, their singly charged counterparts having the same net charge (see Table 2 and

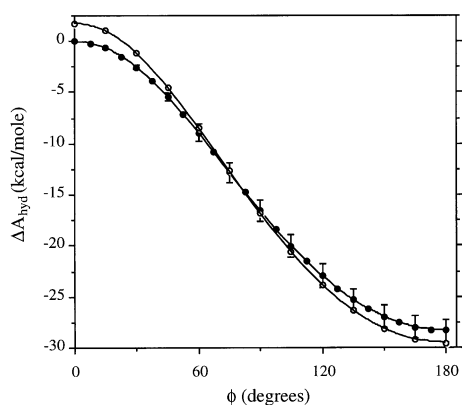


Fig. 5.  $\Delta A_{\text{hyd}}$  of PMPM as a function of  $\phi$ . The closed (●) and open (○) circles are the simulation and continuum model results for PMPM. The simulation results for  $\Delta A_{\text{hyd}}$  are referenced to  $\Delta A_{\text{hyd}}(0^\circ) = 0$ . The continuum predictions have been shifted by an arbitrary constant that minimizes the mean square difference between the simulation and continuum results for  $\Delta A_{\text{hyd}}$ . The simulation error bars correspond to one standard deviation.

Ref. [1]). The *trans* ↔ *gauche* equilibrium constants for both PMPZ and MPMZ are, however, lower than those for PZZZ and MZZZ (e.g.  $K_{\text{MPMZ}} < K_{\text{MZZZ}}$ ). Moreover, the conformational equilibria of PMPZ and MPMZ are not simply the superposition of dipolar and charge interactions, as indicated by the greater stabilization of the *trans* conformations relative to PZZZ and MZZZ, respectively.

The continuum model accurately predicts the free energy profile for PMPZ, but overestimates the free energy difference between the *cis* and *trans* conformations for MPMZ—the predicted  $K_{\text{MPMZ}}$ , however, lies within two standard deviations of the simulation value. The continuum model also correctly predicts that the stabilization of the *trans* conformation of MPMZ is greater than that of PMPZ in water (i.e.,  $K_{\text{MPMZ}} < K_{\text{PMPZ}}$ ). Given the simplifications made in the continuum description of hydration, we conclude that the predicted conformational dependence of the free energy of hydration for MPMZ is reasonable.

### 3.4. PMPM

Compared to the other tetramers, PMPM is unique because its dipole moment changes substantially with  $\phi$ :  $\mu = 4.9$  Debye for the *cis* conformation and  $\mu = 14.7$  Debye for the *trans* conformation. The corresponding decrease in solute volume is, however, inconsequential. Based on Eq. (11), we anticipate that dipolar interactions with water will strongly favor the *trans* conformation of this tetramer. The same mechanism has been applied to explain the conformational equilibrium of 1,2-dichloroethane (DCE) in water [26]. For DCE, however, the dipole moment of the *cis* conformation is greater than that of the *trans* conformation, resulting in the stabilization of the *gauche* conformation. Our expectations are confirmed by the simulation results for PMPM shown in Fig. (5). The free energy of hydration for the *trans* conformation is 28.3 kcal/mol

lower than that of the *cis* conformation,<sup>1</sup> which corresponds to an exceptionally small value for the equilibrium constant:  $2.28 \pm 0.18 \times 10^{-7}$  (Table 2). Thus, the *trans* conformation of PMPM is essentially ‘locked’. The continuum model predicts a similar hydration free energy profile that is in good agreement with the simulation result.

## 4. Conclusions

A comparison of continuum model predictions to results from explicit water simulations of a series of polar and charged flexible polymer chains in water shows that the continuum model of hydration predicts with reasonable accuracy the conformational dependence of the free energy of hydration of these model solutes. In this implementation of the continuum model, the phenomenological parameters inherent to the model are optimized to reproduce the conformational equilibria in water for a subset of the solutes. This subset includes the uncharged tetramer and the two amphiphilic tetramers with either a single positive or negative charge on one terminal methyl group. We also find that both the explicit water simulations and the continuum model give the same ranking of tetramers in terms of their relative *trans/gauche* stabilities in aqueous solution. While this investigation was not exhaustive, our results suggest that the continuum model can be used to discriminate between conformational preferences in water of flexible polymer chains with different sequences of backbone charges.

An unexpected finding of our study is that dipolar interactions stabilize the more compact conformations of the two tetramers with a fixed dipole moment, to an extent greater than hydrophobic interactions. This behavior was observed in the explicit water simulations and predicted by the continuum model. While the simulations gave little insight into the origin of the behavior, the continuum model provided a convenient framework to interpret the observation. In particular, based on Kirkwood’s model of hydration (Eq. 11), we conclude that hydration stabilizes the more compact solute conformations of these dipolar tetramers in order to reduce the cavity volume of the low dielectric solute and gain favorable electrostatic interactions with the high dielectric solvent. This electrostatic driving force for the compact conformation is significant for the tetramers with dipole moments that are fixed, independent of solute conformation; i.e. PMZZ and MPZZ.

Finally, we note that the continuum model is perhaps the simplest implicit treatment of hydration that can successfully capture the observed conformational equilibria in

<sup>1</sup> The GRF self-interaction contribution to the electrostatic energy,  $q_{s_1} q_{s_4} \psi_{\text{GRF}}(r_{s_1, s_4}(\phi))$ , amounts to 8.4 kcal/mol, or about 30% of the *cis* to *trans* hydration free energy difference. Had this contribution not been included in the simulation energy, the agreement between the simulation result and continuum model predictions would have been significantly worse.

aqueous solution. Models based on linear free energy–solute surface area correlations have been developed to describe the hydration of both hydrophobic and polar groups. A surface area-dependent model would fail, however, to predict simultaneously the stabilization of the *trans* conformations for PZZZ and MZZZ, and the *gauche* conformations for PMZZ and MPZZ. Moreover, the change in hydration free energy between the *cis* and *trans* conformations of PMPM is too large to be predicted by a simple, additive surface area correlation.

### Acknowledgements

The authors are indebted to Dr B.L. Neal and Professor A.M. Lenhoff for providing the software used to solve Poisson's equation via the BEM. We are indebted as well to Professor R.J. Zauhar who provided the SMART surface discretization program. Financial support from the National Science Foundation (Grant Nos. BES-9210401 and BES-9510420) and the National Aeronautics and Space Administration (NAG3-1954) is gratefully acknowledged.

### References

- [1] Ashbaugh HS, Kaler EW, Paulaitis ME. *Biophys J* 1998;75:755.
- [2] Wiberg KB, Martin E. *J Am Chem Soc* 1985;107:5035.
- [3] Burkert U, Allinger N. *Molecular mechanics*. Washington, DC: American Chemical Society, 1982.
- [4] Jorgensen WL, Madura JD, Swenson CJ. *J Am Chem Soc* 1984;106:6638.
- [5] Jorgensen WL, Buckner JK. *J Phys Chem* 1987;91:6083.
- [6] Berendsen HJC, Postma JPM, van Gunsteren WF, Hermans J. *Intermolecular forces*. In: Pullman B, editor. *Proceedings of the Fourteenth Jerusalem Symposium on Quantum Chemistry and Biochemistry*. Dordrecht: Reidel, 1981. 331 p.
- [7] Hummer G, Soumpasis DM, Neumann M. *J Phys: Condens Matter* 1994;6:A141.
- [8] Hummer G, Pratt LR, García AE. *J Phys Chem* 1995;99:14188.
- [9] Hummer G, Pratt LR, García AE. *J Phys Chem* 1996;100:1206.
- [10] Garde S, Hummer G, Paulaitis ME. *J Chem Phys* 1998;108:1552.
- [11] Allen MP, Tildesley DJ. *Computer simulation of liquids*. Oxford: Oxford University Press, 1987.
- [12] Owicki JC, Scheraga HA. *Chem Phys Lett* 1977;47:600.
- [13] Zwanzig RW. *J Chem Phys* 1954;22:1420.
- [14] Sitkoff D, Sharp KA, Honig B. *J Phys Chem* 1994;98:1978.
- [15] Ashbaugh HS. PhD dissertation, University of Delaware, 1998.
- [16] Richards FM. *Annu Rev Biophys Bioengng* 1977;6:151.
- [17] Zauhar RJ, Morgan RS. *J Mol Biol* 1985;186:815.
- [18] Jackson JD. *Classical electrodynamics*. 2nd ed. New York: Wiley, 1975.
- [19] Yoon BJ, Lenhoff AM. *J Comput Chem* 1990;11:1080.
- [20] Rashin AA. *J Phys Chem* 1990;94:1725.
- [21] Horvath D, van Belle D, Lippens G, Wodak SJ. *J Chem Phys* 1996;104:6679.
- [22] Pratt LR, Tawa GJ, Hummer G, García AE. *Intl. J Quantum Chem* 1997;64:121.
- [23] Zauhar RJ. *J Comp-Aided Mol Design* 1995;9:149.
- [24] Neal BL. PhD dissertation, University of Delaware, 1997.
- [25] Jorgensen WL. *J Phys Chem* 1983;87:5304.
- [26] Zichi DA, Rossky PJ. *J Chem Phys* 1986;84:1712.
- [27] Kirkwood JG. *J Chem Phys* 1934;2:351.
- [28] Ösabay K, Young WS, Bashford D, Brooks CL, Case DA. *J Phys Chem* 1996;100:2698.